WOOD RESEARCH doi.org/10.37763/wr.1336-4561/67.1.1125
e-ISSN 2729-8906
67(1): 2022 11-25 pp.

ANALYTICAL STUDY ON AXIAL AND ECCENTRIC COMPRESSIVE BEHAVIOR OF POPLAR COLUMN STRENGTHENED BY BFRP

FENGXIA HAN, QING LIU, XIN GUO, MENG ZHANG, XIA HAN
XINJIANG UNIVERSITY
CHINA

(RECEIVED JULY 2021)

ABSTRACT

In this work, the compression behaviour of the Xinjiang poplar column was reinforced by basalt fibre reinforced polymer (BFRP) strips with different reinforced configurations, and the numerical simulations were performed on the axial and eccentric compressions of poplar columns unreinforced and reinforced with BFRP to assess the effect of the bearing capacity and deformation of the columns. The results show that the use of BFRP to reinforce the Xinjiang poplar column effectively improves its axial compressive bearing capacity (axial compression) and bending bearing capacity (eccentric compression), and at the same time, the bearing capacity and stiffness of the columns strengthened by BFRP increased with the bonding area of BFRP.

KEYWORDS: Xinjiang poplar, timber column, BFRP, numerical simulations, compression behavior.

INTRODUCTION

Columns are often used as pressure-bearing members in timber structures, and the Xinjiang poplar in China is also one of the component materials as timber structural members (Hao 2004 and Lü 2001). The poplars growing in Xinjiang are called Xinjiang poplar, which the scientific name is *Populus bolleana* Lauche. The poplars are widely distributed in Xinjiang of China, especially in the south of Xinjiang and Ili River Valley. The poplar has the characteristics of easy reproduction, fast-growing, drought and frost tolerance, little knots, being easy to dry at room temperature (Zeng 2002, Yang 2005, Shu 2005). However, poplar is an anisotropic material (Shen 2013), which has defects, such as natural cracks, and low strength requiring the reinforcement of the Xinjiang poplar members. As a kind of reinforcement material, basalt fiber reinforced polymer (BFRP) composites have the advantages of high strength, lightweight, erosion resistance, corrosion resistance, and convenient construction. Its advantages help to compensate for the deficiencies of the Xinjiang poplar members. Therefore, BFRP is a composite

material suitable for timber structures reinforcement (Sha and Zhu 2012, Chun and Pan 2011, Chen 1995).

Scholars have presented numerous studies on the reinforcement of timber structures. Zhu and Xu (2009), Xu and Zhu (2007) and Zhou et al. (2009) found that the use of carbon fiber reinforced polymer composites to reinforce locally damaged timber columns can restore the compressive bearing capacity and ductility of the columns. Through experimental research on timber columns strengthened with fiber-reinforced polymer composites, some authors (Johns and Lacroixs 2000, Shao et al. 2012, Khelifa et al. 2016) found that the bearing capacity and ductility of the strengthened timber columns were improved to a certain extent. Based on experimental results on timber columns, Khelifa et al. (2015), Sotayo et al. (2016), Zeng et al. (2016) used the timber constitutive model which is based on the elastic theory of small deformation and found that the numerical simulation results are consistent with the experimental results.

The present study on wood structures mainly focuses on strengthening the timber structural members of columns or beams strengthened with fiber cloth based on pine and cedar raw materials by experimental research. The experimental research and numerical simulation analysis of Xinjiang poplar are still relatively limited. Therefore, based on an experiment, numerical simulation is used for finite element analysis to refine and study the mechanical properties of BFRP-strengthened Xinjiang poplar columns.

MATERIAL AND METHODS

Materials

The *Populus bolleana* Lauche material of timber specimens was from Turpan, Xinjiang China. According to GB/T1931 (2009) and GB/T1928 (2009), the moisture content of the sample cut from poplar was tested. The size of the sample was 20 × 20 × 20 mm and continuously dried for 8 hours in a drying oven at 103 ± 2°C. The test result of the poplar moisture content is 10%.

According to GB/T1938 (2009) and GB/T1933 (2009), the density and the tensile and compressive strength tests along the grain of the poplar were obtained as the main mechanical properties. Tab. 1 lists the main properties of the poplar with 10% moisture content.

Tab. 1: Main mechanical characteristics of Xinjiang poplar.

Moisture content (%)	**Density** ($g \cdot cm^{-3}$)	**Tensile strength along grain** (MPa)	**Compressive strength along grain** (MPa)
10.0	4.725	114.4	36.5

The structural adhesive (YZJ-CD), which had a weight ratio of 3:1, was produced by Wuhan Changjiang Reinforcement Technology Co., Ltd in China. The YZJ-CD had a tensile strength of 53.9 MPa, a high elastic modulus of 2885.1 GPa, the axial compression strength of 101.7 MPa, and an elongation of 3.0%. The main performance parameters of the structural adhesive are shown in Tab. 2.

Tab. 2: Properties of structural adhesive.

Tensile strength (MPa)	**Modulus of elasticity** (GPa)	**Axial compression strength** (MPa)	**Elongation at break** (%)
53.9	2885.1	101.7	3.0

The BFRP was acquired from Xinjiang Tuoxin Basalt Fiber Products Co., Ltd in China. The BFRP composite material had a surface density of 360 $g \cdot m^{-2}$, a single fiber diameter of 13 μm, and a thickness of 0.138 mm. The tensile strength, modulus of elasticity, and elongation of the BFRP were 2100 MPa, 105 GPa, and 2.6%, resp. The main mechanical property parameters of BFRP are shown in Tab. 3.

Tab. 3: Mechanical property indexes of BFRP.

Surface density ($g \cdot m^{-2}$)	**Single fiber diameter** (μm)	**Tensile strength** (MPa)	**Modulus of elasticity** (GPa)	**Elongation rate** (%)	**Thickness** (mm)
360	13	2100	105	2.6	0.138

Specimens preparation

Based on the codes of design standard for timber structures (GB50005, 2017) and standard for test methods of timber structures (GB/T50329, 2012), the dimensions of the timber columns were 100 × 100 × 1200 mm for axial and eccentric compression. The initial eccentricity is defined as the distance between the center of the cross-section of the compression column and the point of the external force. 14 axial compression and eccentric compression members were tested respectively. The specific parameters of the specimens are shown in Tab. 4.

Tab. 4: Parameters of Xinjiang poplar long column specimens.

Specimen type	**Specimen number**	**Number**	**Reinforcement method**	**Reinforced with BFRP layers**	**Section size**	**Initial eccentricity** (mm)
Axial compression	DBZ	3	Unreinforced	0	100×100×1200	0
	BJ1	3	BFRP strips with sapcing	1	100×100×1200	
	BJ2	3	BFRP strips with sapcing	2	100×100×1200	
	BM1	3	Fully reinforced by BFRP	1	100×100×1200	
	BM2	3	Fully reinforced by BFRP	2	100×100×1200	
Eccentric compressive	DBZ	3	Unreinforced	0	100×100×1200	100
	BJ1	3	BFRP strips with sapcing	1	100×100×1200	
	BJ2	3	BFRP strips with sapcing	2	100×100×1200	
	BM1	3	Fully reinforced by BFRP	1	100×100×1200	
	BM2	3	Fully reinforced by BFRP	2	100×100×1200	

DBZ - an unreinforced column; in BJn/BMn, *J* - column reinforced by BFRP strips with 50 mm spacing, *M* - fully reinforced by BFRP, *n* - the number of layers about BFRP.

Measurement and loading procedure

In the specimens loading process, the static load method was adopted. In the preloading stage, the load was between 0% and 10% of the ultimate load, each load level was 5 kN, and the load holding time was 3 min. When the load was between10 - 80% of the ultimate load, 10 kN was applied in each load stage, and the load holding time was 3 min. When the load reached 80% of the ultimate load, 4 kN was applied to each stage, also with 3 min of loading duration. When the load limit was reached, the displacement control of the loading method was adopted in the test. The running speed of the experimental machine was controlled at 1.00 $mm \cdot s^{-1}$.

Four linear voltage displacement transducers (LVDTs) (type: YDH-100) were individually arranged in the front, back, left, and right directions of the middle of the specimen to measure the lateral displacement of the specimens. Two LVDTs were arranged vertically to measure the vertical displacement of the specimens. The detailed layout of LVDT is shown in Figs. 1a-e. The detailed layout of strain gauges on each surface of the specimen was shown in Figs. 1f-j.

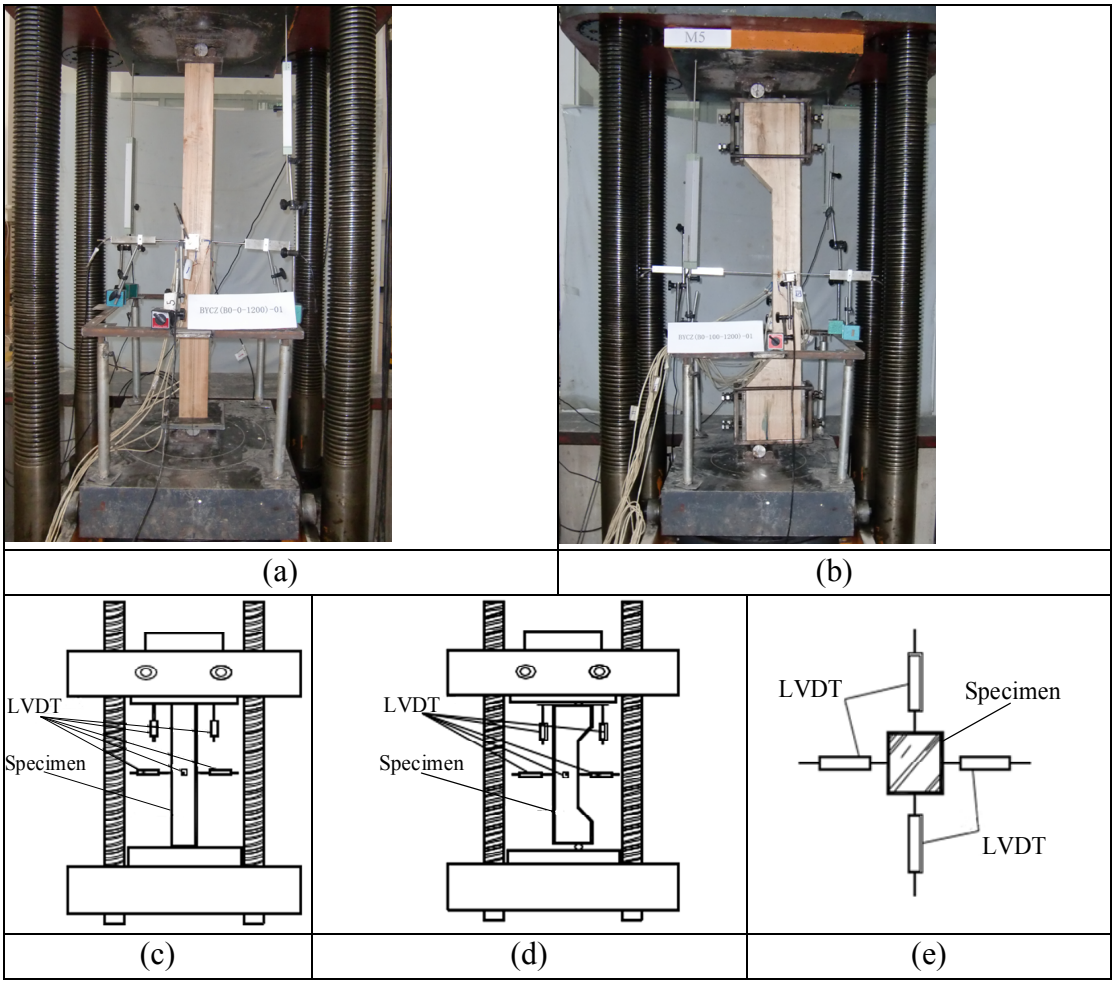

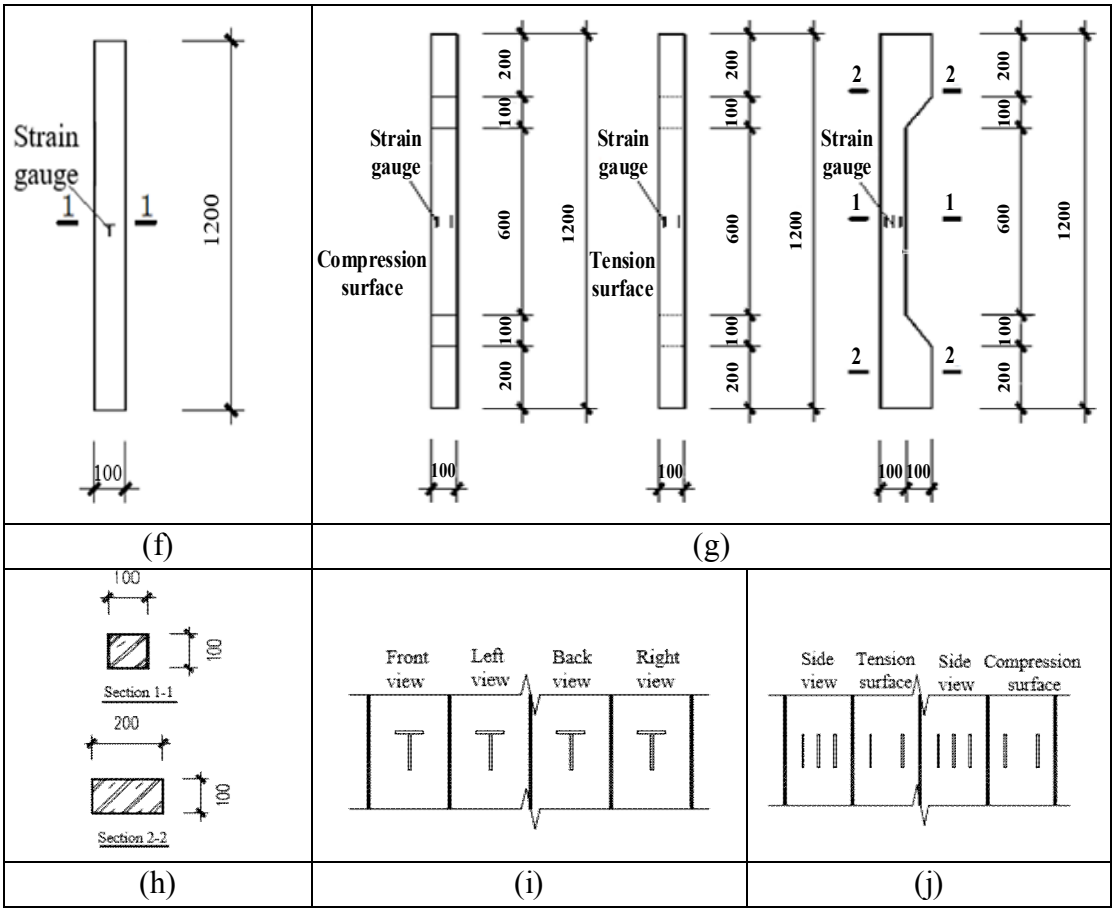

Fig. 1: Layout of measuring points: (a) LVDT arrangement of axial compressive specimen, (b) LVDT arrangement of eccentric compressive specimen, (c) Layout of the axial compressive experiment, (d) Layout of the eccentric compressive experiment, (e) Horizontal layout of LVDT, (f) Paste position and size of strain gauge of axial compressive specimen, (g) Paste position and size of strain gauge of the eccentric compressive specimen, (h) Section size of the specimen, (i) Detailed drawing of strain gauge of the axial compressive specimen, (j) Detailed drawing of strain gauge of the eccentric compressive specimen.

RESULTS AND DISCUSSION

Fracture characteristics

The failure modes of the square timber columns under axial compression are shown in Fig. 2a. The failure modes of the columns are bending failure and the degree of bending failure is different. The distance from the top, middle, and bottom of the damaged timber columns was 300 mm (DBZ), 50 mm (BJn), and 160 mm (BMn) resp. According to observation, it can be found that the failure process of the square timber columns under axial compression was as follows: *(1)* The unreinforced column was basically in the elastic stage when the load was 0-100 kN and the reinforced column was 0-150 kN, exhibiting no fold or other abnormal phenomena in the specimens; *(2)* With the increase of the load, the middle of the unreinforced timber column height was bent, and the timber fiber in the compression zone was crushed, while most of the poplar columns strengthened with the BFRP interval paste were damaged in places without fiber cloth;

increasing folds appeared in the middle of the fully pasted timber columns, and most of the experienced bending failure; *(3)* When the timber columns reached the limit, a fracture appeared at the middle part of the timber column with a sudden sharp "crack" sound. The average ultimate load of the unreinforced timber columns was 126.33 kN. The average ultimate load of the timber columns strengthened by the BFRP interval pastes fiber cloth with 1, and 2 layers and the fully pasted BFRP fiber cloth with 1, and 2 layers and were 160.50 kN, 195.33 kN, 186.50 kN, and 242.00 kN, respectively. Also, It can be seen from Fig. 2a that the bending failure in the middle of the poplar column is a typical failure mode.

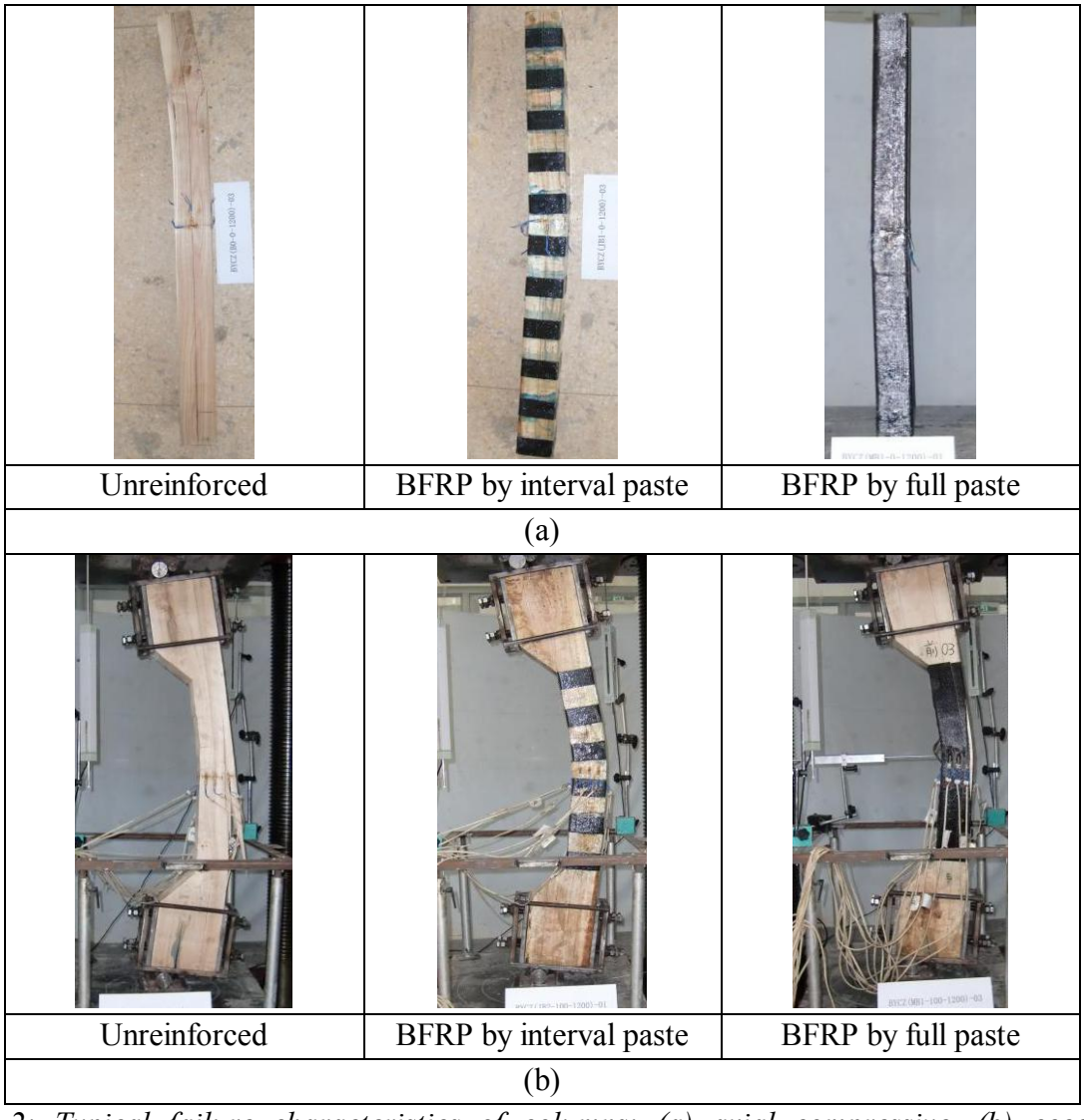

Fig. 2: Typical failure characteristics of columns: (a) axial compressive, (b) eccentric compressive.

The failure mode of the square timber columns under eccentric compression is shown in Fig. 2b. The failure modes of all the columns are bending failure and the phenomenon is very obvious. The damage location was approximately in the middle of the specimen. Its characteristics are mainly described as follows: *(1)* at the beginning of the experiment loading, the load was small, and the horizontal and vertical deformation of the specimen was very small.

At this time, the confined force of the basalt fiber cloth was not produced, and the stress and strain of the specimens were the same as those of the unreinforced column; *(2)* compression cracks first appeared in the middle of the compression surface of the unreinforced specimen with the increase of the load, and the compression area gradually increased with the load. Fig. 2b shows that the ultimate failure of the specimen was caused by the tensile fracture of the timber fiber in the tensile zone, and the cracks at the fracture exhibited a zigzag distribution; *(3)* Fig. 2b indicates that the failure locations in the specimens strengthened by BFRP interval paste were mostly in the unreinforced area, and timber fiber crushing developed into shear failure with a "crackling" sound, displaying a certain suddenness; *(4)* most of the specimens strengthened by BFRP by fully pasting showed a slow development rate of longitudinal flexural deformation, and the fiber cloth was sheared due to the shear failure of the timber fiber in the compression section.

Load-strain response

The load-strain curves of the Xinjiang poplar column specimens strengthened by BFRP are shown in Fig. 3. The load-strain curves of the square columns under axial and eccentric compressions have the same trend, which can be divided into two stages: the elastic and plastic stages. The strain in the elastic stage increased linearly with the load. When the yield load of the specimens was reached, the inflection point of the curve appeared (not obvious, but the slope of the curve decreased gradually), and the strain increased rapidly, but continued to increase linearly until the ultimate load of each specimen was reached. In addition, the comparison of the load-strain curves of the axial and eccentric compression specimens indicates that the strain values of the eccentric columns were significantly greater than those of the axial columns at the same load. However, the ultimate load of the eccentric columns was significantly lower than that of the axial columns, such as the BM2 specimen. The results show that fiber cloth can react against the lateral deformation of timber columns. Also, under the same load and reinforcement method, the strain of the axial compressive column was less than that of the eccentric compressive column, the strain of both axial and eccentric compression specimens increased with the increase of BFRP cloth reinforced lays at the same load.

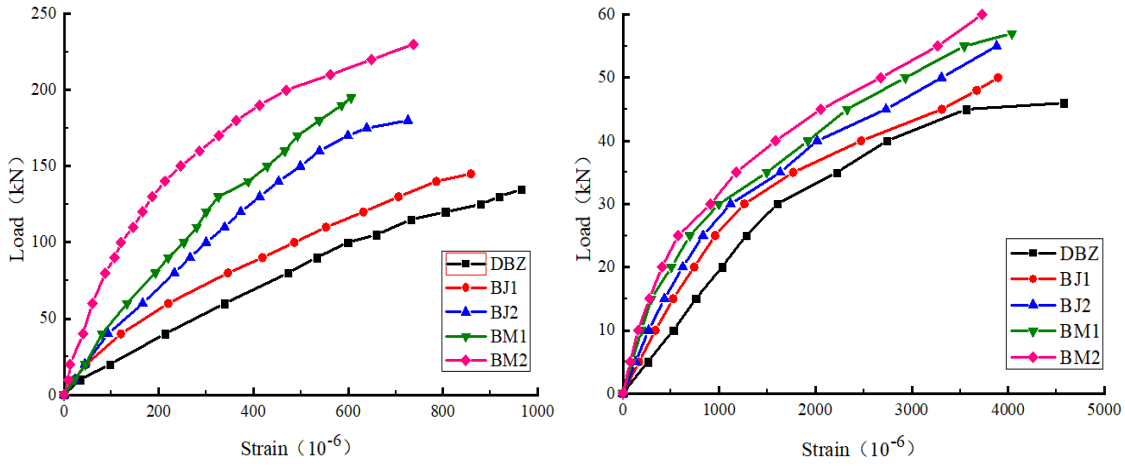

Fig. 3: Load-strain curves: (a) axial compressive, (b) eccentric compressive.

The load-displacement curves of the Xinjiang poplar column specimens are shown in Fig. 4. As can be seen that the load-displacement curve trends of the specimens are the same and can be divided into two stages: the elastic and plastic stages. The displacement in the elastic stage increases linearly with the load.

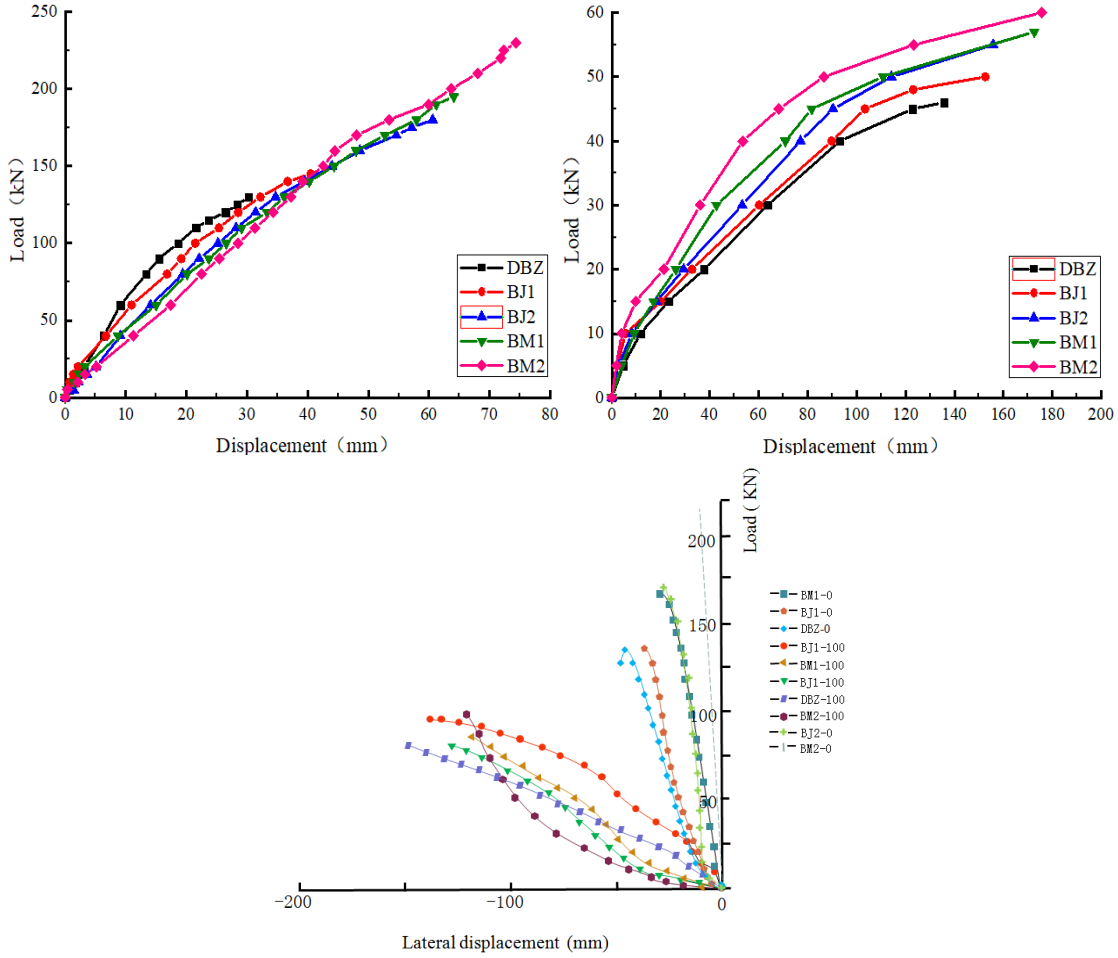

Fig. 4: Load-displacement curves: (a) axial compressive, (b) eccentric compressive, (c) load-lateral displacement curves.

When the yield load of each specimen was reached, an inflection point appeared on the curve. In both axial and eccentric compression columns, the ultimate displacement of the BM2 specimens, which were reinforced with BFRP cloth, reached the maximum value. When the same load and reinforcement method, the displacement of the axial compression column was generally less than that of the eccentric compression column, indicating that the longitudinal deformation capacity of the eccentric column was lower than that of the axial compressive column due to the joint action of the axial force and the bending moment. When the same displacement and reinforcement method, the load of the axial compression column was much higher than that of the eccentric compression column, indicating that the bearing capacity of the eccentric columns was lower than that of the axial columns. The load-lateral displacement curves of the Xinjiang poplar column specimens are shown in Fig. 4c. The lateral displacement of the axial compression columns decrease with the increase of the number of BFRP paste layers,

which demonstrated hoop effects with fiber sheets on the lateral displacement for the specimens. Compared with the unreinforced eccentric compression columns, the lateral displacement of the reinforced eccentric compression columns was decreased and the magnitude of lateral displacement reduction varies with the number of fiber bonded layers. Compared with the axial compression columns, the hoop effect with fiber sheets for the eccentric compression columns is not significant.

Finite element analysis (FEA)

Considering the defects of wood material, the data obtained from the above experiments are quite discrete. To solve this problem, numerical simulation (Hu and Li 2015, Wang 2007) can be used to establish models to simulate the experiment, which is convenient for optimization and accurate for simulating the mechanical properties of structural members.

Stress-strain of materials

Material model of unreinforced Xinjiang poplar

Xinjiang poplar is a kind of heterogeneous and orthotropic material whose constitutive curves can be divided into different stress-strain curves, such as longitudinal tension and compression parallel to the grain, radial tension and compression perpendicular to the grain, and tangential tension and compression, as shown in Fig. 5.

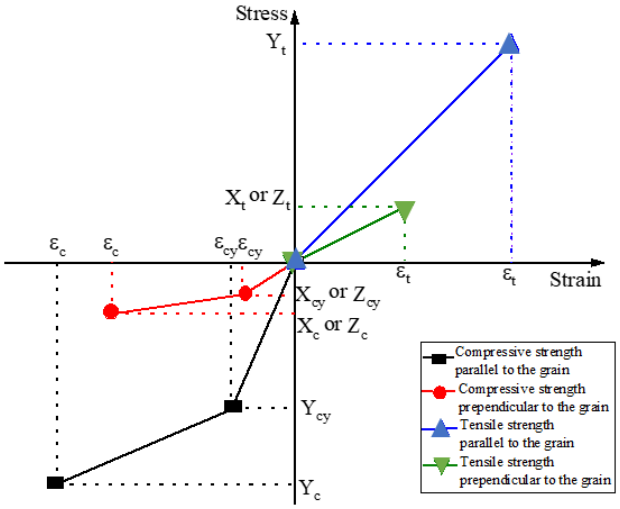

Note: Y_c and Y_{cy} are compressive strength and yield strength parallel to the grain respectively; X_c and Z_c are compressive strength perpendicular to the grain in radial and tangential direction respectively; X_{cy} and Z_{cy} are the yeild compressive strength perpendicular to the grain in radial and tangential direction respectively; Y_t is the tensile strength parallel to the grain; X_t and Z_t are the tensile strength perpendicular to the grain in radial and tangential direction; ε_c and ε_{cy} are compression strain and ultimate strain of timber; ε_t is tension strain of timber.

Fig. 5: Stress-strain curves of Xinjiang poplar.

Wood is a complex anisotropic material (Jeong 2016). In this paper, the orthotropic constitutive relation of the Xinjiang poplar is simplified as transversely isotropic. In the general finite element analysis software ANSYS, the characteristics of the model are as follows:

1) The constitutive relation is orthotropic in the elastic stage and isotropic in the radial and tangential direction, and thus simplified to transverse isotropic. The constitutive relation of poplar in the elastic stage by using the tensor method and the elastic parameters are shown in Tab. 5. *2)* The generalized HILL yield criterion (Chen et al. 2013), which is an anisotropic model for different yield strength in three orthogonal directions of the material, is adopted in the plastic stage. The generalized HILL yield criterion not only considers the difference in yield strength in the three orthogonal directions of the material but also the different yield strengths in the tensile and compressive states. This characteristic is similar to the properties of wood. Thus, the criteria are used as the strength criterion in the plastic stage of Xinjiang poplar. The plastic parameters are shown in Tab. 6. Four independent of each other in three directions of Xinjiang poplar material. The tensile and compressive strength along the grain is different, the tensile and compressive strength perpendicular to the grain is different in the radial direction and the strength perpendicular to the grain is equal to the radial and tangential direction.

Tab. 5: Elastic constitutive parameters of Xinjiang poplar.

EX (MPa)	**EY** (MPa)	**EZ** (MPa)	**PRXY**	**PRYZ**	**PRXZ**	**GXY** (MPa)	**GYZ** (MPa)	**GXZ** (MPa)
900	12600	900	0.12	0.47	0.43	915	732	915

Tab. 6: Plastic constitutive parameters of Xinjiang poplar.

Direction	**X**	**Y**	**Z**
Tensile yield stress (MPa)	2.6	81.2	2.6
Tensile tangent modulus (MPa)	0	0	0
Compression yield stress (MPa)	2.6551	25.4	2.6551
Compression tangent modulus (MPa)	0	3200	0
Shear yield stress (MPa)	5	5	5
Shear tangent modulus (MPa)	0	0	0

Model of Xinjiang poplar reinforced with BFRP

The tensile strength of the BFRP fiber cloth was used in the tests to produce lateral restraint on the timber column. During the experiment, the BFRP fiber cloth was completely in the elastic stage. Therefore, the constitutive model of the Xinjiang poplar column can be obtained by superimposing the elastic constitutive relation of the BFRP and that of the unreinforced Xinjiang poplar column. The BFRP fiber cloth was bonded to the timber column by a structural adhesive. Given the very small thickness of the structural adhesive layer, the influence of the adhesive layer is ignored in this model.

Element applied

The Solid45 element in Fig. 6a is applied to the orthotropic materials in ANSYS and wood is a typical orthotropic material. Thus, the element is used for the wood column. The element was used to construct a three-dimensional solid structure. The element is defined by eight nodes, and each node has three degrees of freedom to translate in the X, Y, and Z directions to match the orthotropic properties of the wood material.

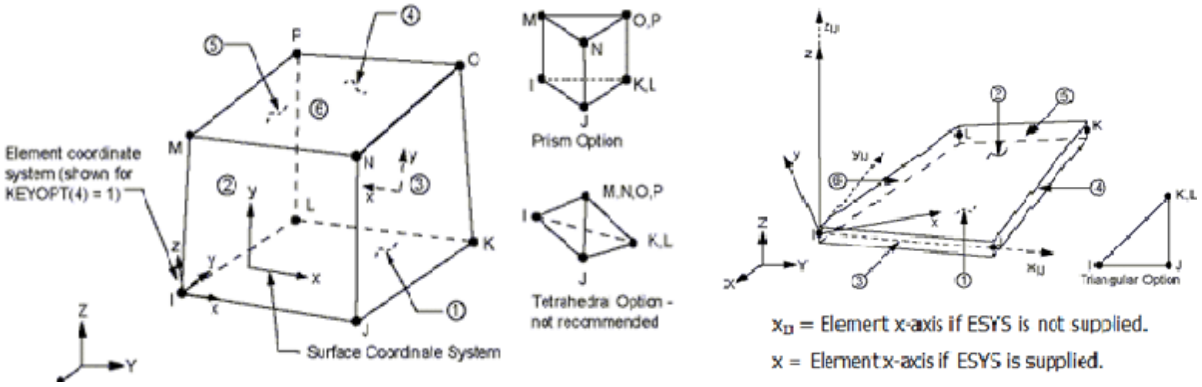

(a) (b)

Fig. 6: Details of finite elements: (a) Solid45, (b) SHELL41.

The SHELL41element in Fig. 6b was applied to mesh the BFRP fiber cloth. The element has large deformation and stress stiffening characteristics. The element is defined by four nodes and each node has three degrees of freedom to translate in the X, Y, and Z directions. The BFRP can be modeled with the SHELL41 element considering the variable thickness and strain strength of the BFRP cloth.

The geometric model meshed with a size of 25 mm of hexahedral mapping, which can satisfy the convergence and accuracy of the modeling results. Boundary and loading conditions were applied to the tested timber column, in which the two ends of the column are the hinged supports, model by restraining the essential nodes to stand for the simply-supported situation.

Comparison of experimental and FEA results

When calculating the models, the initial defect (initial bending) is considered. In this study, the initial defect is set as 1/1000 of the specimen length (i.e. 1.2 mm). The finite element results are shown in Fig. 7, 8, and 9.

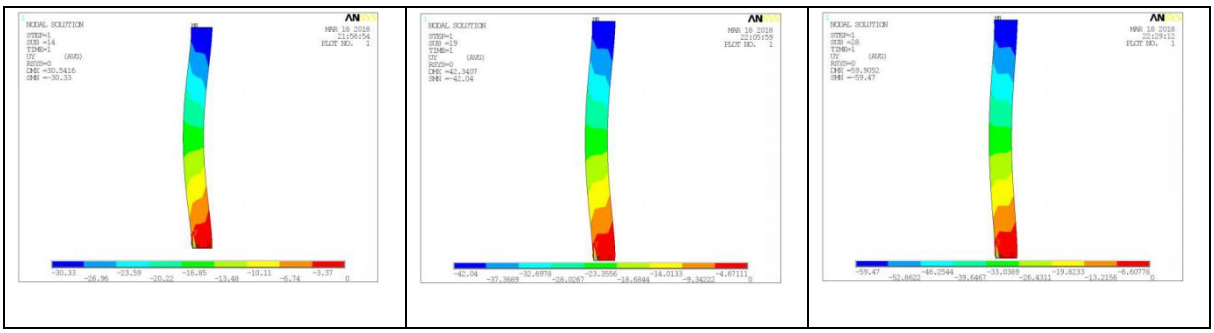

Specimen DBZ Specimen BJ1 Specimen BM1

(a)

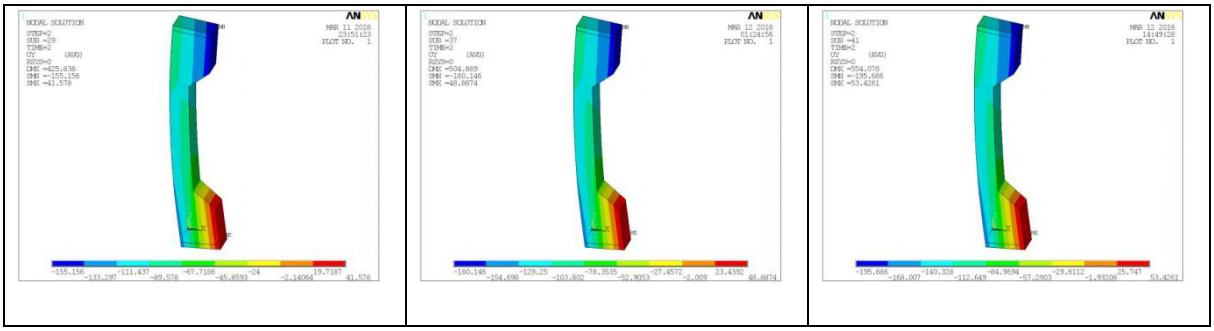

Specimen DBZ Specimen BJ1 Specimen BM1

(b)

Fig. 7: Displacement nephogram of specimens: (a) axial compressive long columns, (b) eccentric compressive long columns.

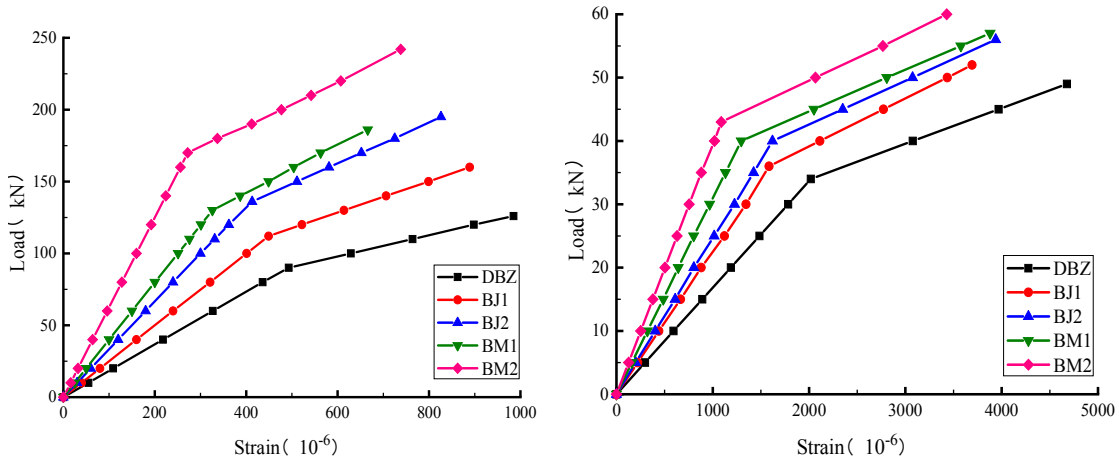

(a) *(b)*

Fig. 8: Load-strain curves of the model columns: (a) axial compressive square columns, (b) eccentric compressive square columns.

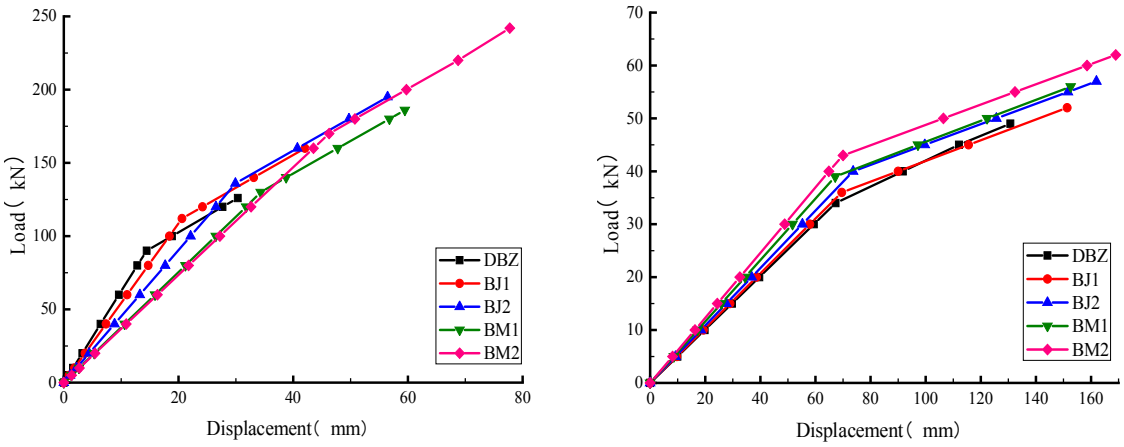

(a) *(b)*

Fig. 9: Load-displacement curves of the model columns: (a) axial compressive square columns, (b) eccentric compressive square columns.

The comparison of the tests and numerical simulation results indicates the following: *(1)* According to the comparison between Figs. 2 and 7, the typical longitudinal bending failure is dominant in the timber column under axial compression, and the timber fiber on the compression side is crushed; the failure mode of the timber column under eccentric compression is mainly longitudinal bending. *(2)* The comparisons between Figs. 3, 4, 8 and 9 indicate the following: *1)* For the timber column, the load-strain curve of each specimen is the same, which can be divided into two stages: the elastic and plastic stages. The displacement of the specimen in the elastic stage increases slowly and evenly with the increasing load. When the yield load is reached, the displacement increases rapidly until the ultimate load of each specimen is reached; *2)* When the BFRP cloth is used to reinforce the timber columns with one layer or two layers of interval and one layer or two layers of full paste, the yield load of the columns under axial compression is increased by 22.2% or 51.1%, and 44.4% or 88.9%, respectively, and the ultimate load increases by 27.0% or 54.8% and 47.6% or 92.1%, respectively; *3)* When the BFRP cloth is used to reinforce the columns with one or two layers of interval and one or two layers of full paste, the yield load of the eccentric compression columns increases by 5.9% or17.6% and14.7% or 23.5%, and the ultimate load of the eccentric compression columns increases by 6.1% or 16.3% and 14.3% or 22.4%, respectively.

The modulus of elasticity of each specimen is calculated according to the load-strain curves at the elastic stage and used as the index in the stiffness analysis (Tab. 7). The stiffness of the Xinjiang poplar columns strengthened by BFRP improved in different degrees compared with the unreinforced columns. The increased range for the axial compression long columns is 35.2%-96.4%, and 9.1%-67.4% for the eccentric compression long columns.

Tab. 7: Percentage of stiffness improvement.

Type	**Number**	**Modulus of elasticity** (MPa)	**Percentage increase in stiffness compared to unreinforced** (%)
Axial compression	DBZ	5097	-
	BJ1	6891	35.2
	BJ2	8122	59.3
	BM1	7891	54.8
	BM2	10011	96.4
Eccentric compression	DBZ	2083	-
	BJ1	2272	9.1
	BJ2	2487	19.4
	BM1	2815	35.1
	BM2	3486	67.4

CONCLUSIONS

In this study, the material model of the Xinjiang poplar was established by ANSYS, and the numerical model of the Xinjiang poplar square and eccentric long columns strengthened by BFRP was established. The load-strain, and load-displacement curves and the bearing capacity with the corresponding experiment results of each specimen were analyzed and compared. The main conclusions are as follows: *(1)* The experimental and numerical simulation results indicate that when the long square columns are reinforced with the same reinforcement method, their

bearing capacity and deformation capacity under axial compression is significantly better than those under eccentric compression. *(2)* The bearing capacity and stiffness of the columns strengthened by BFRP increased with the BFRP bonding area. The bearing capacity and stiffness from low to high follows the order unreinforced, 1 layer BFRP by interval paste, 2 layers BFRP by interval paste, 1 layer BFRP by full paste, and 2 layers BFRP by full paste.

ACKNOWLEDGMENTS

This study was conducted with the support of Natural Science Foundation Youth Regional Fund (51708479) and Xinjiang Uygur Autonomous Region (2019D01C028). The authors declare that they have no competing interests.

REFERENCES

1. Chen, L., Wen, W.D., Cui, H.T., 2013: Generalization of Hill's yield criterion to tension-compression asymmetry materials. Science China Technological Sciences 56(1): 89-97.
2. Chun, Q., Pan, J.W., 2011: Experimental study on mechanical properties of timber columns strengthened with CFRP/AFRP hybrid FRP sheets under axial compression. Journal of Building Materials (in Chinese) 14: 427-431.
3. Chen, Y.S., 1995: Maintenance guide of ancient buildings and wooden relics: Protection of timber structures in ancient buildings. China Forestry Press (in Chinese). Beijing, 180 pp.
4. GB/T1931, 2009: Methods for determination of wood moisture content.
5. GB/T1928, 2009: General test methods for wood physics and mechanics.
6. GB/T1933, 2009: Method for determination of the density of wood.
7. GB/T 1938, 2009: Method of testing in tensile strength parallel to grain of wood.
8. GB50005, 2017: Design standard for timber structures.
9. GB/T50329, 2012: Standard for test methods of timber structures.
10. Hao, C.R., 2004: Looking at the prospects of Chinese wood structure building from the development of Chinese and western wood structure buildings. Master's Thesis. Tsinghua University.
11. Johns, K.C., Lacroixs, S., 2000: Composites reinforcement of timber in bending. Canadian Journal of Civil Engineering 27: 899-906.
12. Jeong, G.Y., Park, M.J., 2016: Evaluate orthotropic properties of wood using digital image correlation. Construction and Building Materials 113: 864-9.
13. Khelifa, M., Celzard, A., Oudjene, M., Ruelle, J., 2016: Experimental and numerical analysis of CFRP strengthened finger-jointed timber beams. International Journal of Adhesion and Adhesions 68: 283-297.
14. Khelifa, M., Lahouar, M.A., Celzard, A., 2015: Flexural strengthening of finger-jointed Spruce timber beams with CFRP. Journal of Adhesion Science and Technology 29: 2104-2116.

15. Lü, J., 2001: Studies on adaptability of *Populus bolleana* and other poplar trees in northwest Shanxi Province. Journal of Forestry Research12(1): 31-34.
16. Shen, G.L., 2013: Mechanics of Composite Materials. Tsinghua University Press (in Chinese), Beijing, 343 pp.
17. Shao, J.S., Xue, W.C., Liu, W.Q., Jiang, J.Q., Jiang, T., 2012: Calculation of axial compressive behavior of timber column laterally strengthened with FRP. China Civil Engineering Journal 45(8): 48-54.
18. Sha, Z., Zhu, X.D., 2012: Literature review of the research on wood structure strengthened by FRP. Forest engineering (in Chinese) 28: 57-61.
19. Shu, Q.L., Chen, C.Y., Zhang, H., Sun, Q., Zhang, X., 2005: Investigation of the species, occurrence character and control measures of poplar diseases in Anhui province. Journal of Anhui agricultural sciences (in Chinese)33(7) : 1193-1195.
20. Sotayo, A., Green, S., Turvey, G., 2016: Experimental and finite element (FE) modelling of timber fencing for benchmarking novel composite fencing. Composite Structures 158: 44-55.
21. Wang, X.M., 2007: Numerical analysis of ANSYS engineering structure. China Communications Press (in Chinese). Beijing, 554 pp.
22. Xu, Q.F., Zhu, L., 2007: An experimental study on partially-damaged wood columns re-paired and strengthened with CFRP. China Civil Engineering Journal (in Chinese) 8: 41-46.
23. Yang, Z.J., 2005: Wood structure-green energy-saving building structure. Building Energy Conservation 33(3): 50-52.
24. Zeng, D.P., 2002: Research status and control of poplar disease in China forest pests. Forest Pest and Disease (in Chinese) 21(1): 20-26.
25. Zhou, Q., Yan, W.M., Li, Z.B., Ji, J.B., 2009: Study on strengthening methods of timber structures of ancient buildings. Earthquake Resistant Engineering and Retrofitting (in Chinese) 31(01): 84-90.
26. Zhu, L., Xu, Q.F., 2009: Experimental research on short cracked timber columns strengthened with CFRP. Building structure (in Chinese) 11: 101-103.
27. Zeng, D., Zhou, X.Y., Cao, L., 2016: Research on the mechanical properties of larch glulam columns under axial compression. Industrial Construction (in Chinese) 46: 63-67, 71.

FENGXIA HAN*, QING LIU*, XIN GUO, MENG ZHANG, XIA HAN
XINJIANG UNIVERSITY
SCHOOL OF ARCHITECTURAL AND CIVIL ENGINEERING
XINJIANG, 830047
CHINA
*Corresponding authors: csjjj02@sina.com and liuqing2666@163.com